

A prestorage method to measure neutron transmission of ultracold neutron guides

B. Blau^a, M. Daum^a, M. Fertl^{a,b,1}, P. Geltenbort^c, L. Göttl^{a,b}, R. Henneck^a, K. Kirch^{a,b}, A. Knecht^a, B. Lauss^{a,*}, P. Schmidt-Wellenburg^a, G. Zsigmond^a

^aPaul Scherrer Institute (PSI), CH-5232 Villigen PSI, Switzerland

^bInstitute for Particle Physics, Eidgenössische Technische Hochschule (ETH), Zürich, Switzerland

^cInstitute Laue-Langevin (ILL), 71 avenue des Martyrs, F-38000 Grenoble, France

Abstract

There are worldwide efforts to search for physics beyond the Standard Model of particle physics. Precision experiments using ultracold neutrons (UCN) require very high intensities of UCN. Efficient transport of UCN from the production volume to the experiment is therefore of great importance. We have developed a method using prestored UCN in order to quantify UCN transmission in tubular guides. This method simulates the final installation at the Paul Scherrer Institute's UCN source where neutrons are stored in an intermediate storage vessel serving three experimental ports. This method allowed us to qualify UCN guides for their intended use and compare their properties.

Keywords: ultracold neutron, neutron transmission, neutron transport, neutron guide, ultracold neutron source

PACS: 28.20.Gd, 28.20.-v, 29.25.Dz, 61.80.Hg

1. Introduction

Ultracold neutrons (UCN) are defined via their unique property of being reflected under any angle of incidence from the surface of suitable materials with high material optical potential V_F (Fermi potential) [1, 2]. This is only occur-

*Corresponding author, bernhard.lauss@psi.ch

¹Now at University of Washington, Seattle WA, USA.

ring for neutrons with very low kinetic energies in the neV range, corresponding to velocities below 7 m/s or temperatures below 3 mK. Hence their name "ultracold". Well-suited materials are e.g. stainless steel, Be, Ni, NiMo alloys or diamond-like carbon which display total UCN reflection up to their respective V_F of 190, 252, 220 or 210 - 290 neV, respectively [1, 2]. Closed containers of such materials can confine UCN and serve as UCN storage vessels. Evacuated tubes or rectangular shaped guides made of or coated with materials of high V_F can be used to transport UCN over distances of several meters.

The ultracold neutron source at PSI [3–7] is now in normal operation. About ten meters of neutron guides are necessary to transport UCN from the intermediate storage vessel to one of the three beam ports, traversing the several meter thick biological shield. The UCN guides, made from coated glass or coated stainless steel, are housed inside a stainless steel vacuum system. High vacuum conditions are required in order not to affect the UCN storage and transport properties.

The main thrust for the construction and operation of high intensity UCN sources [8] comes from the needs of high precision experiments like the search for a permanent electric dipole moment of the neutron [9–11]. Efficient transport of UCN from production to the experiment is a necessity. In addition, installation of the guides is a complex and lengthy procedure. Moreover, the replacement of a guide would cause a long shutdown. Therefore, it was decided to install only UCN guides tested with UCN and with known good UCN transmission. We have developed the prestorage method, described in section 2, which allowed us to perform a quality check on UCN guides and a quantification of the UCN transmission properties before final installation.

1.1. UCN transmission

Ignatovich [2] dedicates a long chapter in his book to "Transporting UCN" and gives the definition of UCN transmission as "the transmission of a neutron guide is the ratio of UCN flux at the output to the flux at the input". This is applicable when regarding continuous UCN sources and continuous experiment

operation. In storage type experiments, when an experimental chamber has to be filled within a given time period and using a UCN source with UCN intensity decreasing with time, the integrated number of UCN and the UCN passage time is relevant. In our method the transmission of the time-integrated counts will be studied instead of the flux transmission.

Independent of the materials used, UCN transmission increases with guide diameter and decreases with guide length L . For comparison between different types of guides the normalized transmission per meter (T_{norm}) is used. The total guide transmission T then follows as:

$$T = (T_{\text{norm}})^{\frac{L}{1\text{m}}}. \quad (1)$$

Fig. 1 shows the calculated behavior of the UCN transmission with increasing guide length for normalized UCN transmissions in a realistic range for good UCN guides. A length of about 10m is necessary at the PSI source to pass the biological shielding. Fig. 1 demonstrates the importance of even small improvements in UCN transmission for such long installations. In general, the properties of the materials and UCN exposed surfaces, are decisively separating the good and the bad guides.

In the past, various measurements have been made to define and measure the properties of UCN guides with early attempts summarized in [2]. The topic is also treated in recent publications [12–16], but experiments have notoriously been difficult with results not-necessarily transferable to other measurements. Problematic issues were necessary assumptions on neutron flux, neutron energy distribution, detector efficiencies, and reproducibility of installations concerning e.g. small gaps in the setup causing UCN losses.

Assuming a single number for UCN transmission is a simplification as the transmission probability depends on the kinetic energy and angular distribution of the neutrons. Furthermore, it is important to know how fast UCN traverse the guide, i.e. how fast one can fill an experiment on the exit side, which directly correlates to specular reflectivity and integral transmission. In principle it would be possible to repeat our measurements with monoenergetic UCN with a more

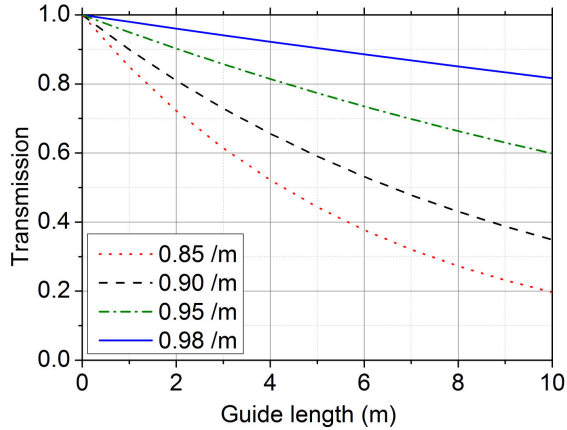


Figure 1: Calculated transmission probability of UCN through a guide with increasing length for different normalized transmission probabilities between 0.85 /m and 0.98 /m

complicated setup.

The main parameters which define the neutron transmission of a UCN guide can be summarized as follows:

- Surface roughness: The total reflections of neutrons from surfaces can be classified in specular reflections, where the angle of incidence is co-planar and equals the reflection angle and diffuse reflections, where the reflection angle is independent of the incident angle and follows a cosine distribution with respect to the perpendicular direction [1]. This simple view is valid for roughness values much larger than the neutron wavelength. For very low roughness, e.g. for highly polished copper or coated glass surfaces [17], diffraction effects become important and the probability of diffuse reflections will depend on the incident angle and neutron elocity (see also [2]). The influence of surface roughness on UCN reflection has been studied recently in detail using flat plates as reflector [18]. High UCN transmission is obtained with negligible diffuse reflections. which results in a short passage times for the UCN through the guide. Hence, low surface roughness is a main quality criterion with glass being the preferential material.

- Material optical potential V_F : The coherent neutron scattering length and material density defines the absolute value of V_F which determines the energy range where total UCN reflection under any angle of incidence occurs [2]. A high value of V_F therefore allows to transmit UCN with higher energies and hence increases the UCN intensity.
- Neutron losses via material interaction: UCN reflect from surfaces at any angle of incidence in case their kinetic energy is below V_F . As described by an imaginary part of the potential [1], there is a small probability that the UCN undergoes nuclear capture during reflection due to the neutron wave-function which slightly penetrates the surface barrier. The UCN losses are therefore energy dependent.

In addition, the UCN can also inelastically scatter from surface atoms or impurity atoms sticking to the surface [19]. Wall temperatures always exceed UCN temperatures, causing UCN acceleration out of the UCN regime via phonon scattering. The overall loss due to these surface effects can be parametrized by a “loss-per-bounce” coefficient as a ratio of the imaginary and real parts of the optical potential. This coefficient is independent on kinetic energy. From this and the kinetic energy of the UCN one can calculate the loss per bounce probability μ by using Eq. (2.68) in [1]. An energy-averaged loss per bounce probability μ_{av} can be estimated by transmission measurements. For the extraction of the loss-per-bounce coefficient one needs to know the energy spectrum and the angular distribution of the UCN.

- Gaps: The passage of UCN through a guide can be regarded similar to the propagation of an ideal gas. Gaps and holes, necessary e.g. for vacuum pumping, represent direct loss channels during UCN transport according to their relative surface area. In addition, areas of low V_F which are directly visible to UCN also represent leaks, e.g. at positions where surface coating is missing. Avoiding gaps and holes is therefore of great importance in order to achieve a high UCN transmission.

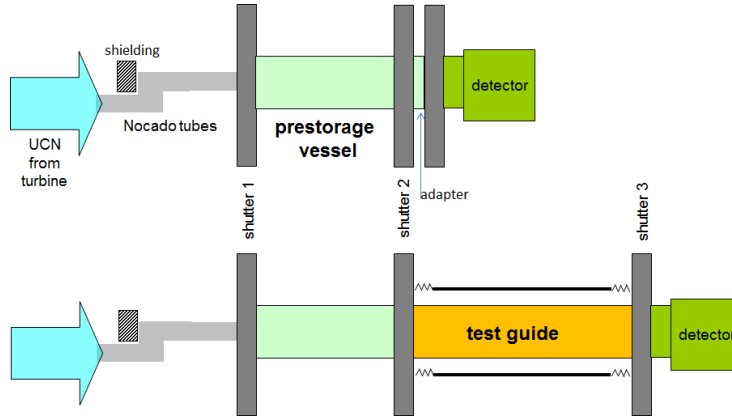


Figure 2: Sketch of the prestorage measurement setup: a) calibration measurement; b) test guide measurement.

2. The prestorage method to determine UCN transmission

The setup for the prestorage measurement is sketched in Fig.2. A prestorage vessel is filled with a defined and known number of UCN in a vessel prior to their release into a sample guide or directly into the detector. These stored UCN can then be directly measured with a detector mounted onto the vessel and hence be used as calibration. Then, an additional UCN guide - the one to be tested - is mounted between the prestorage vessel and the detector and the measurement is repeated. The comparison of the integrated UCN counts in the two measurements is defined as the UCN transmission through the test guide for the given UCN energy spectrum.

This measurement setup resembles a small version of the PSI UCN source setup, where the neutrons may also be stored in an intermediate storage vessel. All UCN with kinetic energies above the material optical potential will be rapidly lost during storage, defining a reproducible energy spectrum. The prestorage vessel also influences the momentum direction distribution due to diffuse reflections. UCN passing long UCN guides have momenta peaked along the direction of the guide axis [2]. After a sufficiently long storage period – of tens of seconds – this peak is largely reduced.

A similar approach to determine guide transmission was followed by [20] for a longer and geometrically more complicated UCN guide. This measurement and analysis was criticized by [2] as an invalid method. The criticism is based on the fact that the prestorage vessel in the experiment was emptied through a small orifice, thus, the experiment was mainly comparing the storage time of the vessel, the outflow time and the measurement time. The fact that in our case the geometry is much simpler, i.e. the diameter of the UCN guide is not reduced in comparison to the storage vessel and there are no bends in the setup, makes the method primarily sensitive to the UCN transmission of the guide. Besides a simple analysis, our measurements can be used to tune Monte Carlo simulations in order to describe realistic guide performances [7, 21].

2.1. Experimental setup

Our experiment was carried out at the PF2 facility of the Institut Laue-Langevin (ILL) using the EDM beamline of the UCN-turbine [22]. UCN are typically guided from the turbine port towards the experiment using electro-polished stainless steel tubes manufactured by Nocado². The filling line included two 90° bends, which allow for an accurate setup alignment and significantly decrease the amount of UCN with kinetic energies above the material optical potential of steel. The Nocado tubes used have an inner diameter of 66 mm. At the end of the guides, the UCN enter the prestorage vessel through a stainless steel adapter flange mounted on customized vacuum shutters, special DIN-200 shutters from VAT³ with inside parts coated with diamond-like carbon [19, 23–25] (see Sec.2.3). These shutters were later installed as beam ports of the PSI UCN source.

The measurement setup consists of a prestorage unit and a detection unit, which both remain unchanged during the measurements. In the calibration measurement a stainless steel adapter connects these two units (Fig.2a). An

²Nocado GmbH & Co. KG, Kirchweg 3, 26629 Groefehn, Germany

³VAT Vakuumventile AG, Seelistrasse, 9469 Haag, Switzerland

additional test guide is mounted between these units in a transmission measurement. (Fig.2b).

The prestorage unit is confined by shutter 1 and shutter 2. The storage vessel is a tube made from DURAN[®]⁴, a borosilicate glass, with 180 mm inside diameter, 5 mm wall thickness. The tubes are sputter-coated⁵ on the inside with about 400 nm of nickel-molybdenum (NiMo), at a weight ratio of 85 to 15, an alloy with a Curie temperature well below room temperature [26]. The use of the same surface coating in the prestorage vessel as in the guides shapes the UCN energy spectrum in a suitable way.

The detector unit consists of a similar VAT shutter (No. 3) which is only used as a connector unit to the 2D-200 CASCADE-U detector⁶ via a 150 mm long NiMo coated glass guide contained in a vacuum housing. The Cascade-U detector is a gas electron multiplier (GEM)-based UCN detector using a 200 nm thin-film of ¹⁰B deposited on the inside of the 0.1 mm AlMg3 entrance window of the detector to convert UCN to two charged particles (α and ⁷Li). These particles ionize the detector gas⁷. The charge is amplified by the GEM foils and detected by a pixelated readout structure. The sensitive area of the detector covers the inner diameter of the glass guides [7].

2.2. Measurement sequence

Our standard sequence for transmission measurements has the following scheme:

- Wait for the UCN turbine signal (shutter 1 open, shutter 2 closed);
- Fill the storage vessel for an optimized filling time of 30 s;
- Close shutter 1;
- Store UCN for a preset storage time of 5 s;

⁴SCHOTT AG, Hattenbergstr. 10, 55122 Mainz, Germany

⁵S-DH GmbH Heidelberg, Sputter-Dünnschichttechnik, Hans-Bunte-Strasse 8-10, 69123 Heidelberg, Germany

⁶CDT CASCADE Detector Technologies GmbH, Hans-Bunte-Strasse 8-10, 69123 Heidelberg, Germany

⁷Typically we used as counting gas Ferromix, a mixture of 18% CO₂ and 82% Ar.

- Open shutter 2;
- Count UCN as a function of arrival time in the detector;
- Close shutter 2 after the measurement time;
- Open shutter 1 and wait again for UCN.

Shutter 3 stays permanently open during the entire measurement sequence and functions in transmission measurements only as connector piece. However, it is used in storage measurements.

2.3. Shutter properties

The large VAT shutters used have opening/closing times of about 1 s. The prestorage method is sensitive to the precise timing of shutter operations. We therefore measured the timing properties and the shutter opening function which influences the path of the UCN and their arrival at the detector.

The shutter body is made of aluminum containing a moving part with a round opening and closing disc. All parts seen by UCN in the open and closed position, or during movement are coated with DLC. When the closing disc is retracted, the 25 mm gap at the center of the shutter is covered by an expanding ring to close the gap. Fig. 3 shows the VAT opening displaying the frame of the moving part in an intermediate position. The shutter is air-actuated and controlled with electric valves.

We have measured the timing between the closing of shutter 1 and opening of shutter 2. This time defines the UCN storage time and hence the number of neutrons released into the sample. Its accuracy is crucial for the reproducibility of the measurements.

In a separate measurement with similar conditions concerning actuating pressure and environmental temperature we determined without neutrons the relative timing stability of shutter 1 and 2. The time of the shutter end-switch signals with respect to the slow control start signal was measured. The resulting time differences were filled into a histogram with 1 ms bins, shown in Fig 4. Note that the experiment was set to have exactly 5 s time difference which was accurate on the 10^{-3} level. The standard deviation σ of a Gaussian fit is 3.2 ms,

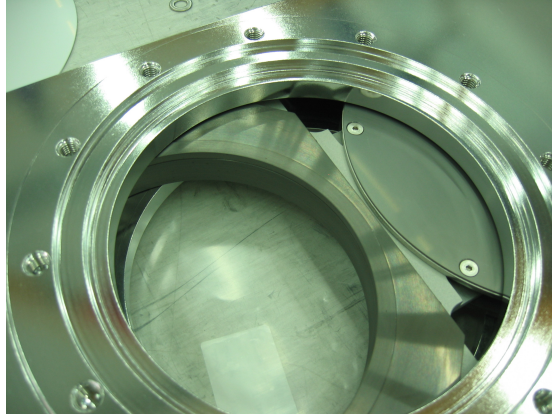


Figure 3: VAT shutter opening showing the insert frame with opening hole and closing disc in an intermediate position while moving.

reflecting an excellent reproducibility of the opening and closing times.

The opening of the shutter also partially obstructs the path of the UCN during the movement, which is reflected in the opening function. We used a bright lamp and a camera for the measurement of the light transmission passing or deflecting on the intercepting shutter parts, supposing a comparable opening function for light and UCN. Fig.5 shows a selected sequence of pictures showing the shutter during opening. Fig.6 shows the resulting opening function measured with three different actuator pressure settings of 3, 5, and 7 bar. No significant difference was observed for the different pressures.

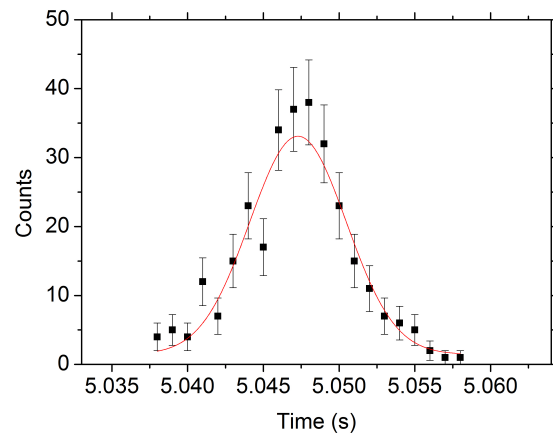


Figure 4: Histogram of the time difference between the closed signal from shutter 1 and the open signal from shutter 2. The red line shows a Gaussian fit with a standard deviation of 3.2 ms.

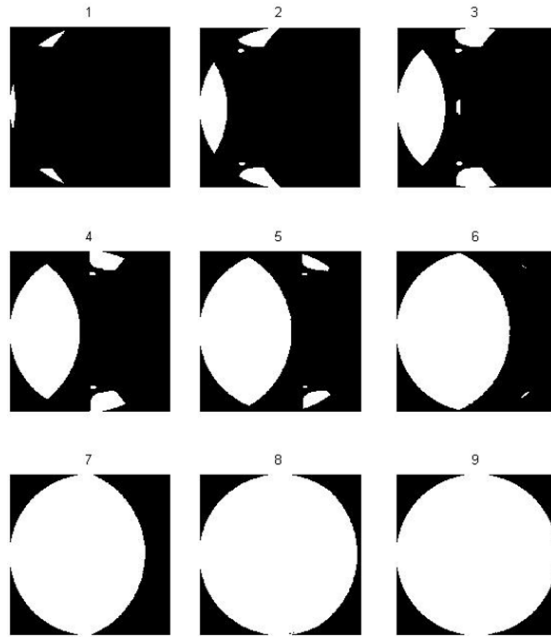


Figure 5: Nine selected pictures showing the opening of the VAT shutter. Opening function of the VAT shutter, 1 - just after opening; 3 - the main obstructive part of the shutter holder is visible in the center of the opening; 9 - the shutter is fully open.

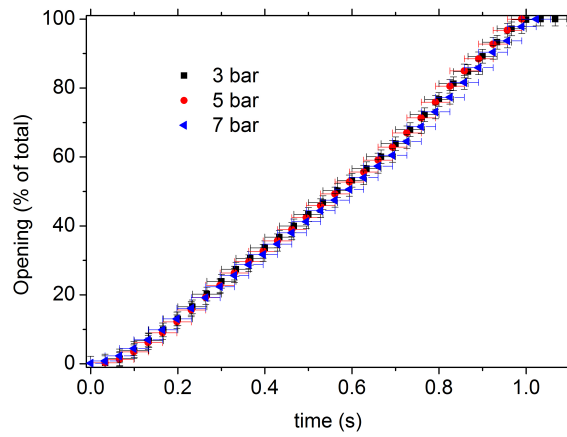


Figure 6: Opening function of the VAT shutter – given in percent of total opening – measured with three different actuator pressures of 3, 5 and 7 bar.

2.4. Calibration setup

The standard calibration setup is used to determine the UCN transmission through the setup without a test guide. The detection unit is connected to the prestorage vessel using a special adapter, a 60 mm short stainless steel piece. In order to optimize the transmission properties for the UCN and to minimize the influence of this adapter on the measurement, it was made as short as possible and the inner surface was hand-polished.

In addition, the standard setup was modified in such a way that shutter 3 and the stainless steel adapter were removed. By comparing the results from the standard calibration measurement and the modified calibration measurement one obtains the influence of the stainless steel flange on the total count rate. In section 3.3.1 we show these measurements agree within statistical uncertainties. Hence, the influence of the adapter can safely be neglected.

2.5. Setup for transmission measurement

A photo of the setup installed at the ILL EDM beamline for the transmission measurements is shown in Fig.7. The test guides were mounted in a custom vacuum housing between shutters 2 and 3. As all the guides were designed to be installed at the PSI UCN source short adapter pieces had to be manufactured in order to connect the guides to the VAT shutters in the transmission measurements. All adapter pieces were made of stainless steel with a maximal length of 40 mm. The inside surfaces which act as neutron guides were hand polished to have negligible influence on the transmission measurements.

Care was taken to minimize any possible gaps between guides and adapters. Two flexible bellows at both ends of the vacuum housing setup allowed to adapt the vacuum housing length to the total guide and adapter length.

Table 1 states names, lengths and materials of the measured guides. Their names refer to the subsequent placement at the PSI UCN source which is shown in Fig.9. The given guide lengths include the stainless steel end flanges which are permanently glued to the glass guide [27] to allow for a stable connection

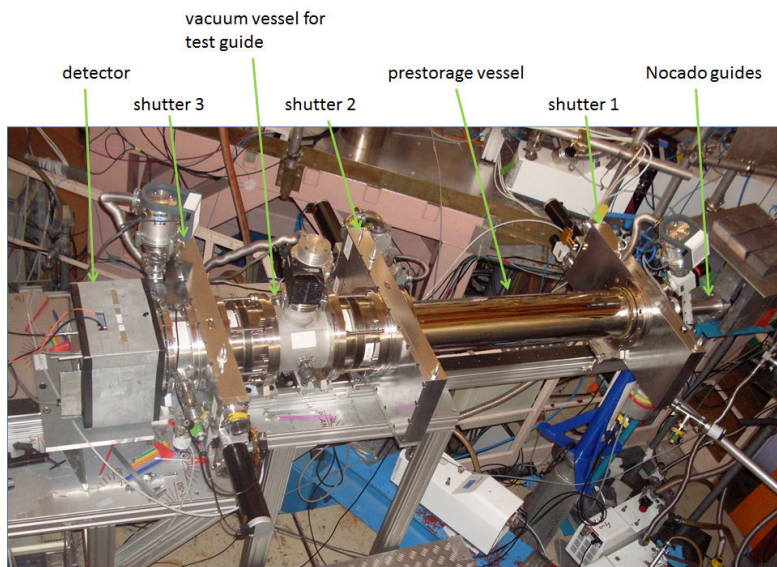


Figure 7: Photograph showing the setup installed at the EDM beamline at ILL for the measurement of the guide 1S3. The Cascade detector (in cadmium shielding) with shutter-3, the prestorage vessel with shutter 1 and 2. Behind shutter 1 are the Nocado filling guides hardly visible.



Figure 8: View of the UCN butterfly valve in open (a) and half closed (b) position.

and minimal gap widths between various parts in the final installation at PSI. In addition, the total length includes the additional stainless steel adapter.

All guides have inner diameters of 180 mm, only the guides 2W1 and TA-W2 have inner diameters of 160 mm. All guides, glass and stainless steel, were coated on the inside with the same NiMo coating with a weight ratio of 85 to 15 percent which is non-magnetic at room temperature. The small section with the UCN butterfly valve shown in Fig. 8 is coated with diamond-like carbon (DLC). Guides 1S1 and 1W3 are similar guides with identical dimensions and properties.

Due to the large dimensions of the setup and the high weight of the components, accurate alignment was critical in order not to damage the equipment. The prestorage unit, all vacuum vessels for the tested guides, the VAT shutters, and the detector unit were all mounted on custom made carriages that could be moved on a Hepco GV3 rail system ⁸. Thus, a precise alignment of the components with respect to each other could be achieved.

All measurements were performed at vacuum pressures below 10^{-3} mbar.

⁸Hepco Motion Lower Moor Business Park, Tiverton, Devon, United Kingdom

Guide name	Material	Total length	Guide length	Glass length	Inside diameter
		(mm)	(mm)	(mm)	(mm)
1W1	glass	2624	2565.7	2498.7	180
1W2	glass	2351	2344	2320	180
2W1	glass	1655	1597	1530	160
1S1	glass	3783	3725	3658	180
1S2	glass	2628	2621	2597	180
1S3	glass	603	575	543	180
TA-W1	st.steel	1024	900	-	180
TA-W2	st.steel	1024	900	-	160

Table 1: Guide names and corresponding lengths. Names refer to locations for final mounting in the UCN source setup. The given guide lengths include the NiMo coated stainless steel flanges glued onto the glass guides. The total lengths include also the stainless steel adapter pieces necessary to mount the guides in the setup. The material column defines the material of the tube, namely glass or stainless steel. The stainless steel guides include the part with the neutron valve. 1S1 and 1W3 are similar guides with identical dimensions and properties.

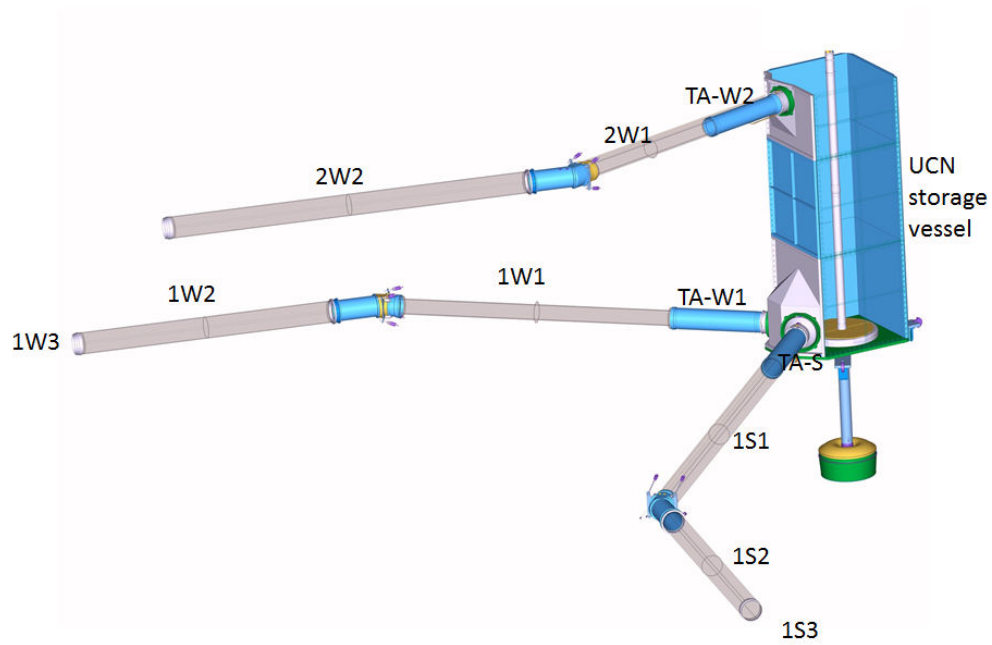


Figure 9: Drawing of some parts of the UCN source relevant for this paper, showing the UCN storage vessel (about 2.5 m high) and the three UCN guide sections towards the experimental ports West-1, West-2 and South with the naming scheme for the corresponding guide parts. The green vessel displays the container for the solid deuterium used for UCN production. All the shown parts are contained in a large vacuum tank [5, 6]

3. Optimization of the measurement

To investigate and optimize the experimental conditions systematically it is useful to divide it into three steps which are repeated several times in a cycle:

1. Filling UCN into the prestorage vessel.
2. Storing UCN in the prestorage vessel.
3. Releasing the UCN out of the vessel via the test guide to the detector.

In order to start every measurement from the same initial conditions shutters 1 and 2 were closed before step 1. Triggered by the turbine signal the opening of shutter 1 started the filling phase, thus allowing the UCN density in the storage vessel to build up. Shutter 1 closed after the filling time. During the subsequent storage phase the UCN energy spectrum shifts to a lower mean value due to velocity dependent losses, i.e. for UCN energies larger than the material optical potential of the material trap and because of losses on the material surface (loss-per-bounce) at different bounce rates [1, 2].

Once the storage time had elapsed, shutter 2 was opened, allowing the remaining UCN to move freely in the combined volume of the prestorage vessel, the test guide, and the detector unit where they are counted. Although, most UCN penetrate the AlMg3 detector window, a small fraction is initially reflected and may be counted at later times.

3.1. Filling time

In order to maximize the amount of UCN per cycle the filling time of the prestorage vessel was optimized. We define the filling time between the beginning of the filling process, i.e. the signal from the turbine, and the electronic signal to the shutter triggering its closing motion. After a scan of different shutter 1 closing times 30s was chosen as the working point for all measurements.

In order to understand possible systematic effects in the filling phase, one has to pay attention to the fact that the UCN turbine at ILL is a multi-user facility [22]. It serves three main beam ports sequentially, i.e. there is a UCN guide inside the turbine which is moved by a stepping motor towards the port that

has requested UCN. Once the guide is pointed at one port, the user working at that port obtains an electronic signal to confirm the guide position. However, the UCN density in the guide-part up to the port builds up with time, thus, making the UCN density up to shutter 1 a function of the position of the distributing guide prior to the electronic signal.

In the process of the data analysis we noticed a difference in the number of UCN depending on the position of the turbine prior to the beginning of a measurement cycle. The effect was noticed twice but may have happened more often. For the known occasions where the turbine pattern changed during a measurement period the effect amounts to 0.007 of the total number of UCN detected. The data acquisition system used for the experiments added the data of subsequent cycles until stopped by the user, alas, most measurements were done in long over-night runs without attendance. Thus, the data may contain cycles with either reduced or increased numbers of UCN. Due to the fact that all the cycles are superimposed of the DAQ system used in these runs, it is impossible to separate the cycles and the turbine position imposes a relative systematic uncertainty of up to 0.007 on all measurements. This uncertainty dominates the uncertainty budget of the entire experiment. As will be shown later in section 4 the transmission values are consistent and the uncertainty described here could well be an overestimation.

3.2. Storage time

The duration of the storage phase determines the shaping of the energy spectrum of the UCN that will be measured.

To quantify the storage properties of the prestorage vessel the storage time constant (STC) was determined from a single exponential fit to the data. We define the storage time to be the time that elapses between the electronic signal closing shutter 1 and the signal opening shutter 2. Figure 10 shows the measurements together with a single exponential fit resulting in a STC of 18.5 ± 0.5 s. The storage curve is rather poorly defined by the fit because it neglects the energy dependence of UCN storage. However, for an estimation of the systematic

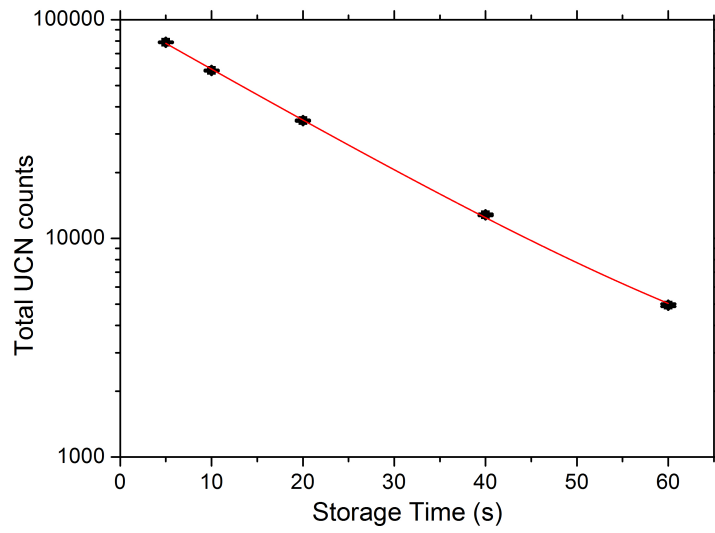


Figure 10: The total UCN counts as a function of the storage time in the prestorage vessel. A fit with a single exponential results in a storage time of 18.5 ± 0.5 s.

uncertainty it is sufficient.

In order to estimate the systematic uncertainty of the number of stored UCN we use the STC from the single exponential fit and the measured rate of the filling time which is ~ 130 UCN/s at 30s of filling time. The relative uncertainty of 0.053 s^{-1} from the measured filling rate is a function of the timing uncertainty mainly due to control electronics and shutter movement. Using $\text{FWHM} = 7.6 \text{ ms}$ of the shutter timing as uncertainty of the storage time the corresponding relative uncertainty in UCN counts computes to $0.053 \times 0.0076 = 4 \cdot 10^{-4}$.

3.3. Emptying the prestorage vessel

3.3.1. The calibration measurement

To investigate the influence of the stainless steel adapter used in the calibration setup a dedicated measurement was performed. The detector unit was mounted directly onto shutter 2, removing shutter 3 and the stainless steel adapter. However, this largely increases the time necessary for a setup change. Figure 11 shows a comparison of the time distribution of UCN counts arriving after shutter 2 opening. The slight difference in the shape of the two curves can be explained by a 30% difference in length of two flight paths behind shutter 2. Using all recorded measurement cycles the mean values of the total number of UCN detected in the modified setup, 69595 ± 52 , and in the standard calibration setup, 69577 ± 60 , agree within statistical uncertainty. One can conclude that the influence of the stainless steel adapter on the obtained transmission values is negligible.

In order to check for systematics and long term drifts the calibration setup was (re)assembled and measured at several occasions throughout the campaign. The results from the measurements performed on the 17.04. and 23.-24.04., as shown in Fig. 12, differ by 0.4% in the mean number of UCN counted per cycle. Fluctuations of UCN intensity due to changes in cold source performance or reactor power of 0.5% are not unusual. In between the two measurements the entire setup, except the detection unit, was taken apart and reassembled.

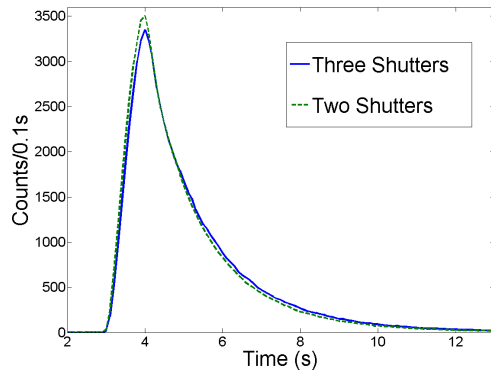


Figure 11: Comparison of emptying curves for the two setups, calibration setup with 3 shutters and adapter (standard calibration setup), and calibration setup with shutter 3 removed. The plotted UCN counts after shutter opening shows the sensitivity of the setup towards a rather small change in length which causes a small change in arrival time.

The agreement of the two measurement periods demonstrates the level of reproducibility of the setup. The measurements taken on the 20.04. were taken under vacuum conditions in the 10^{-2} mbar range. This data points towards the necessary vacuum conditions for measurements and is not used for the calculation of the mean number of UCN per calibration cycle.

Averaging over all calibration measurements performed on April 17, 23, and 24, one obtains a mean number of 78292 ± 68 UCN per calibration cycle used in the further analysis.

3.3.2. Transmission measurements of glass guides

All measurements were taken with the Cascade-U detector in time-of-flight (TOF) mode, i.e. the slow-control started the detector one second before shutter 2 was opened. The emptying curve of the experiment was recorded with a time resolution of 1 ms and re-binned by a factor of 10 in the analysis.

Figure 13 shows emptying curves for different glass guide lengths. One can clearly see the effect of increasing distance between prestorage vessel and detection unit: the rising edge of the spectrum starts at a later point in time and

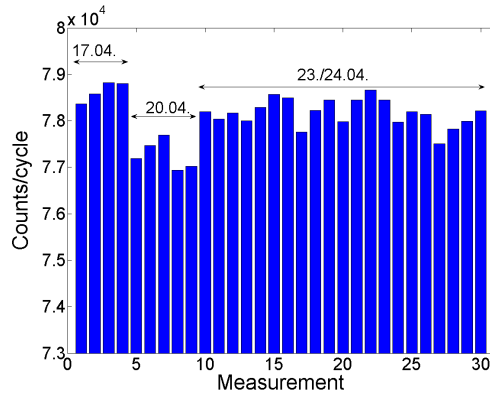


Figure 12: Mean number of UCN over time for different calibration measurement cycles. The data was taken on four different days, in between the indicated dates the experiment was disassembled and reassembled, thus indicating the reproducibility of the obtained results. Measurements from 20.04. were taken under inferior vacuum conditions and not further used in the analysis.

becomes less steep; the falling edge becomes longer with the length of the guide.

3.4. Transmission measurements of stainless steel tubes

The first meter of each of the three UCN guides at the PSI UCN source, dubbed “TA”, is made of hand-polished and NiMo coated stainless steel [5, 7]. It also contains a DLC-coated UCN butterfly valve shown in Fig.8 which can control the neutron flux towards the experimental area. Two of the three stainless steel units (West 1 and West 2) were tested at ILL in the same way as the guides. The measurements were done twice for each unit with varying tilt angle of the UCN valve. Figure 14 shows the dependence of the UCN counts on the angle of the UCN butterfly valve.

It is interesting to see that up to a tilt angle of $\sim 45^\circ$, the decrease of the UCN counts only amounts to $\sim 10\%$, while the “covered” cross-sectional area at this angle corresponds to about 70% of the entire guide.

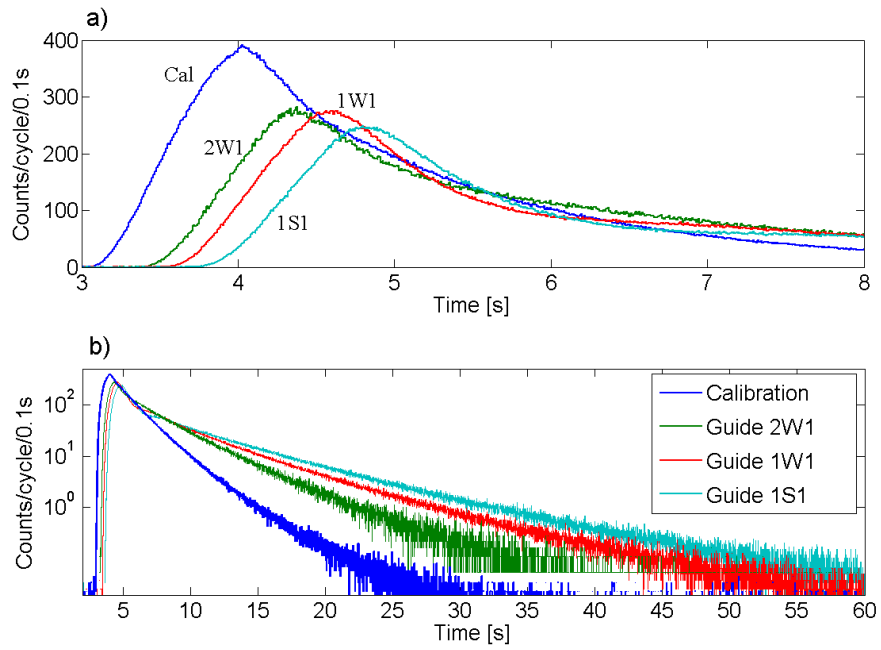


Figure 13: Glass guide measurements: Emptying time spectra for the calibration setup and the transmission setup with guides 1S1, 1W1 and 2W1. a) up to 7s after the beam kick; b) up to 60s. The spectra show a prompt peak which contains most of the UCN and a long tail which contains UCN which have undergone many reflections. In the longest guide UCN are stored up to one minute before being counted in the detector.

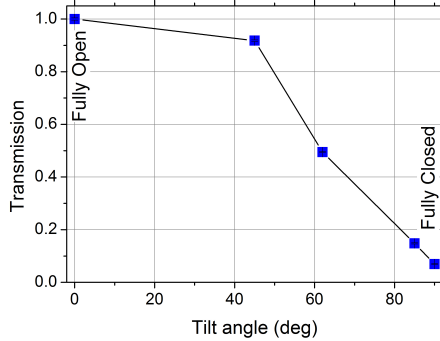


Figure 14: The dependence of UCN counts on the tilt angle of the UCN butterfly valve. The valve is rotated around its axis in the middle of the guide, hence, when fully open only the thickness of the disc (~ 3 mm) blocks the path of the neutrons over the entire guide diameter. Even when fully closed a few percent of UCN leak through the not perfectly closing valve. Statistical errors are smaller than the symbol size. The line is for eye-guiding only.

3.5. Normalized UCN transmission

To allow for a quality check of the guide's surfaces and coatings and a better comparison between the individual guides, the transmission per meter of guide T_{PM} is calculated as follows:

$$T_{PM} = \left(\frac{Counts_{\text{Guide}}}{Counts_{\text{Calibration}}} \right)^{\frac{1}{L}} \quad (2)$$

where $Counts_{\text{Guide}}$ and $Counts_{\text{Calibration}}$ are the mean total number of counts detected per measurement cycle with the test guide or the calibration setup respectively, and L is the length of the tested guide in meters.

4. Results and Discussion

4.1. Results from the individual measurements

All measurements were taken in the time-of-flight mode, however, the transmission is calculated from the mean total of UCN counts in a given setup, i.e. the integral of the TOF spectrum. Table 2 gives the average numbers of UCN counted per cycle for the respective setups. The uncertainty given in Tab. 2 is

Setup name	Counts per cycle	number of cycles
Calib. April	78292±68	19
1W1	75791±91	8
1W2	76719±149	3
2W1	75763±68	18
1S1	74098±216	4
1S3	76323±80	3
Calib. Oct.*)	74927±48	42
1S2*)	74817±38	60

Table 2: Measurement results for glass guides: Mean number of counts per cycle with statistical uncertainty only, obtained with the different setups. The measurements marked with *) were performed in October. The difference in calibration counts points towards a different performance of the UCN turbine or feeding line, as the reactor power was within 0.5% the same as in April.

the statistical uncertainty. The last column states the number of cycles used for the calculation of the mean and standard deviation. The larger cycle numbers occurred in undisturbed overnight runs.

Table 3 shows the results from the stainless steel guide measurements.

4.2. Estimate of the systematic uncertainties

There are several sources for systematic uncertainties in this experiment.

- The timing uncertainty can be estimated conservatively from our measured filling rate of ~ 130 UCN/s at 30 s of filling time. Hence, even the large assumption of a UCN shutter timing jitter of 1 s results in a relative uncertainty of the total number of UCN per cycle of < 0.0002 .

The DAQ and electronics for the shutter movement have been tested separately and have shown to be reproducible to a level of better than 10 ms (Fig. 4) resulting in a relative systematic uncertainty on the level of 10^{-5} .

Setup name	Counts per cycle	number of cycles
Calib. September	70613±24	138
TA-W1 open	69592±37	62
TA-W1 closed	3888±8	32
TA-W2 open	68678±22	182
TA-W2 closed	4779±21	14

Table 3: Results for stainless steel guides: Mean number of UCN counts for the given setups. The difference in calibration counts points towards a different performance of the UCN turbine or feeding line, as the reactor power was within 0.5% the same as in April.

- As described in section 3.1 the effect of the turbine UCN guide moving to different positions imposes a relative uncertainty of 0.007 on all measurements. However, this is an upper limit as the measurements typically average over several different positions of the turbine UCN guide.
- The relative systematic uncertainty arising from the duration of the UCN storage amounts to $4 \cdot 10^{-4}$ (Sec. 3.2).
- We estimate the relative systematic uncertainty from the reproducibility of the calibration measurement from Fig. 12 to be on the order of 0.004.
- Due to the fact that the glass tubes used are not machined to very high precision, gaps with typical sizes of 0.1 to 0.2 mm, occurred in the guide measurement setup. Accurately measuring the impact of those gaps on the UCN counts is very difficult. In Sec. 3.3.1 it was demonstrated that a 60 mm stainless steel adapter and a complete VAT shutter can be removed without affecting the number of detected UCN, hence, we concluded that estimated gaps outside the storage vessel of about 0.5 mm, over the entire circumference of the guide, have a negligible influence on our transmission result.
- The reactor power is monitored and was stable to $\sim 0.2\%$ over the measurement period. Hence, the influence on the measurement results is neg-

Source	Impact
Filling stop time	$< 10^{-5}$
Turbine position	0.0070
Storage phase	0.0034
Calibration	0.0040
Total	0.0081

Table 4: Summary of estimated values for considered relativ systematic uncertainties on the measured count integrals.

ligible.

After carefully analyzing the data, we quote the results with separate statistical and systematic uncertainties. The systematic uncertainty is dominated by the turbine positioning. All relative contributions summarized in table 4 were added quadratically (0.0081) and then increased to 0.0085 for a conservative estimate. A relative systematic uncertainty of 0.012 follows for all quoted transmission values.

4.3. UCN transmission using the calibration measurement

Using the numbers from Tab. 2 and Tab. 3 we obtain the transmission values of Tab. 5 for the UCN spectrum emerging from the prestorage vessel after 5 s of storage.

The results show a remarkable performance of the glass guides. Assuming the guides to have equal properties except their length one can calculate a mean transmission per meter of 0.989 ± 0.012 .

The transmission values obtained for the stainless steel guides are given in Tab. 6. In case of TA S-1 only the straight guide without the valve was measured and behaved as TA W-1 given in Tab. 6.

Guide name	Total transmission	Transmission per meter
1W1	0.968(1)(12)	0.988(1)(12)
1W2	0.980(2)(12)	0.991(2)(12)
2W1	0.968(1)(12)	0.980(1)(12)
1S1	0.946(3)(12)	0.986(3)(12)
1S2	0.999(1)(12)	0.999(1)(12)
1S3	0.975(1)(12)	0.959(1)(12)

Table 5: Transmission values for the glass UCN guides. The uncertainties given are statistical and systematical respectively.

Guide name	Total transmission
TA W-1 open	0.986(6)(12)
TA W-1 closed	0.055(3)(12)
TA W-2 open	0.973(4)(12)
TA W-2 closed	0.068(3)(12)

Table 6: Transmission values for the stainless steel UCN guides. Open and closed refers to the UCN valve position. The uncertainties given are statistical and systematical respectively. The total length of guide, valves and adapters are almost exactly 1 m.

5. Summary

We have developed and used a prestorage method to determine UCN transmission of tubular UCN guides.

Most importantly, the measurements provided a quality control for the UCN guides prior to their installation at the PSI UCN source.

The results show excellent UCN transmission of the investigated guides. The measurements have shown that all guide tubes have transmission values above 95% per meter. The glass guides, which are dominantly used in the PSI UCN source, have transmissions above 98% per meter.

6. Acknowledgements

This work is part of the Ph.D. thesis of L. Göttl. We would like to thank all people which contributed to design and construction of our experiment. A. Anghel, P. Bucher, U. Bugman, M. Mähr and the AMI shop, F. Burri, M. Dubs, J. Ehrat, M. Horisberger, R. Knecht, M. Meier, M. Müller and his shop, T. Rauber, P. Rüttimann, R. Schelldorfer, T. Stapf, J. Welte (all PSI); T. Brenner (ILL); F. Lang, H. Häse (S-DH); J. Städler (GlasForm Gossau); M. Klein (C-DT). TU Munich (E18) allowed the use of their table installed at PF2. Support by the Swiss National Science Foundation Projects 200020_137664 and 200020_149813 is gratefully acknowledged.

References

- [1] R. Golub, D. Richardson, S. Lamoreaux, *Ultra-Cold Neutrons*, Adam Hilger, Bristol, Philadelphia, and New York, 1991.
- [2] V. Ignatovich, *The Physics of Ultracold Neutrons*, Clarendon, Oxford, 1990.
- [3] A. Anghel, F. Atchison, B. Blau, B. van den Brandt, M. Daum, R. Doelling, M. Dubs, P.-A. Duperrex, A. Fuchs, D. George, L. Göttl, P. Hautle,

- G. Heidenreich, F. Heinrich, R. Henneck, S. Heule, T. Hofmann, S. Joray, M. Kasprzak, K. Kirch, A. Knecht, J. Konter, T. Korhonen, M. Kuzniak, B. Lauss, A. Mezger, A. Mtchedlishvili, G. Petzoldt, A. Pichlmaier, D. Reggiani, R. Reiser, U. Rohrer, M. Seidel, H. Spitzer, K. Thomsen, W. Wagner, M. Wohlmuther, G. Zsigmond, J. Zuellig, K. Bodek, S. Kistryn, J. Zejma, P. Geltenbort, C. Plonka, S. Grigoriev, The psi ultra-cold neutron source, *Nuclear Instruments and Methods in Physics Research Section A* 611 (2009) 272–275.
- [4] B. Lauss, A new facility for fundamental particle physics: The high-intensity ultracold neutron source at the Paul Scherrer Institute, *AIP Conference Proceedings* 1441 (1) (2012) 576–578.
- [5] B. Lauss, Startup of the high-intensity ultracold neutron source at the Paul Scherrer Institute, *Hyperfine Interactions* 211 (2012) 21–25.
- [6] B. Lauss, Ultracold Neutron Production at the Second Spallation Target of the Paul Scherrer Institute, *Physics Procedia* 51 (2014) 98.
- [7] L. Göttl, Characterization of the PSI ultra-cold neutron source, Ph.D. thesis, ETH Zürich, No.20350 (2012).
- [8] K. Kirch, B. Lauss, P. Schmidt-Wellenburg, G. Zsigmond, Ultracold neutrons - physics and production, *Nucl. Phys. News* 20:1 (2010) 17–23.
- [9] C. Baker, G. Ban, K. Bodek, M. Burghoff, Z. Chowdhuri, M. Daum, M. Fertl, B. Franke, P. Geltenbort, K. Green, M. van der Grinten, E. Gutmiedl, P. Harris, R. Henneck, P. Iaydjiev, S. Ivanov, N. Khomutov, M. Kasprzak, K. Kirch, S. Kistryn, S. Knappe-Gruneberg, A. Knecht, P. Knowles, A. Kozela, B. Lauss, T. Lefort, Y. Lemiere, O. Naviliat-Cuncic, J. Pendlebury, E. Pierre, F. Piegsa, G. Pignol, G. Quemener, S. Rocchia, P. Schmidt-Wellenburg, D. Shiers, K. Smith, A. Schnabel, L. Trahms, A. Weis, J. Zejma, J. Zenner, G. Zsigmond, The search for the neutron electric dipole moment at the paul scherrer institute, *Physics Procedia*

17 (0) (2011) 159 – 167, 2nd International Workshop on the Physics of fundamental Symmetries and Interactions - PSI2010.

- [10] S. Afach, C. Baker, G. Ban, G. Bison, K. Bodek, M. Burghoff, Z. Chowdhuri, M. Daum, M. Fertl, B. Franke, P. Geltenbort, K. Green, M. van der Grinten, Z. Grujic, P. Harris, W. Heil, V. Helaine, R. Henneck, M. Horras, P. Iaydjiev, S. Ivanov, M. Kasprzak, Y. Kermaidic, K. Kirch, A. Knecht, H.-C. Koch, J. Krempel, M. Kuzniak, B. Lauss, T. Lefort, Y. Lemiere, A. Mtchedlishvili, O. Naviliat-Cuncic, J. Pendlebury, M. Perkowski, E. Pierre, F. Piegsa, G. Pignol, P. Prashanth, G. Quemener, D. Rebreyend, D. Ries, S. Roccia, P. Schmidt-Wellenburg, A. Schnabel, N. Severijns, D. Shiers, K. Smith, J. Voigt, A. Weis, G. Wyszynski, J. Zejma, J. Zenner, G. Zsigmond, A measurement of the neutron to ^{199}Hg magnetic moment ratio, *Physics Letters B* 739 (2014) 128–132.
- [11] S. Afach, G. Ban, G. Bison, K. Bodek, M. Burghoff, M. Daum, M. Fertl, B. Franke, Z. Grujic, V. Helaine, M. Kasprzak, Y. Kermaidic, K. Kirch, P. Knowles, H.-C. Koch, S. Komposch, A. Kozela, J. Krempel, B. Lauss, T. Lefort, Y. Lemiere, A. Mtchedlishvili, O. Naviliat-Cuncic, F. Piegsa, G. Pignol, P. Prashanth, G. Quemener, D. Rebreyend, D. Ries, S. Roccia, P. Schmidt-Wellenburg, A. Schnabel, N. Severijns, J. Voigt, A. Weis, G. Wyszynski, J. Zejma, J. Zenner, G. Zsigmond, Constraining interactions mediated by axion-like particles with ultracold neutrons, *Physics Letters B* 745 (2015) 58–63.
- [12] V. Nesvizhevsky, Polished sapphire for ultracold-neutron guides, *Nuclear Instruments and Methods in Physics Research Section A: Accelerators, Spectrometers, Detectors and Associated Equipment* 557 (2) (2006) 576–579.
- [13] C. Plonka, P. Geltenbort, T. Soldner, H. Haese, Replika mirrors - nearly loss-free guides for ultracold neutrons - measurement technique and first

preliminary results, Nuclear Instruments and Methods in Physics Research Section A 578 (2) (2007) 450–452.

- [14] I. Altarev, A. Frei, P. Geltenbort, E. Gutmiedl, F. Hartmann, A. Mueller, S. Paul, C. Plonka, D. Tortorella, A method for evaluating the transmission properties of ultracold-neutron guides, Nuclear Instruments and Methods in Physics Research Section A 570 (1) (2007) 101–106.
- [15] A. Frei, K. Schreckenbach, B. Franke, F. Hartmann, T. Huber, R. Picker, S. Paul, P. Geltenbort, Transmission measurements of guides for ultracold neutrons using UCN capture activation analysis of vanadium, Nuclear Instruments and Methods in Physics Research Section A 612 (2) (2010) 349–353.
- [16] M. Daum, B. Franke, P. Geltenbort, E. Gutmiedl, S. Ivanov, J. Karch, M. Kasprzak, K. Kirch, A. Kraft, T. Lauer, B. Lauss, A. Mueller, S. Paul, P. Schmidt-Wellenburg, T. Zechlau, G. Zsigmond, Transmission of ultracold neutrons through guides coated with materials of high optical potential, Nuclear Instruments and Methods in Physics Research Section A 741 (0) (2014) 71–77.
- [17] A. Steyerl, Effect of surface roughness on the total reflexion and transmission of slow neutrons, Zeitschrift für Physik A Hadrons and Nuclei 254 (1972) 169–188, 10.1007/BF01380066.
- [18] F. Atchison, M. Daum, R. Henneck, S. Heule, M. Horisberger, M. Kasprzak, K. Kirch, A. Knecht, M. Kuzniak, B. Lauss, A. Mtchedlishvili, M. Meier, G. Petzoldt, C. Plonka-Spehr, R. Schelldorfer, U. Straumann, G. Zsigmond, Diffuse reflection of ultracold neutrons from low-roughness surfaces, The European Physical Journal A 44 (1) (2010) 23–29.
- [19] F. Atchison, T. Brys, M. Daum, P. Fierlinger, P. Geltenbort, R. Henneck, S. Heule, M. Kasprzak, K. Kirch, A. Pichlmaier, C. Plonka, U. Straumann, C. Wermelinger, G. Zsigmond, Loss and spinflip probabilities for ultracold

- neutrons interacting with diamondlike carbon and beryllium surfaces, *Phys. Rev. C* 76 (4) (2007) 044001.
- [20] P. Ageron, W. Mampe, R. Golub, J. Pendelbury, Measurement of the ultra cold neutron production rate in an external liquid helium source, *Physics Letters A* 66 (6) (1978) 469–471.
- [21] Z. Chowdhuri, G. Zsigmond, MCUCN, Proceedings ICANS XIX, 2010 Grindelwald, Switzerland.
- [22] A. Steyerl, H. Nagel, F.-X. Schreiber, K.-A. Steinhauser, R. Gaehler, W. Glaeser, P. Ageron, J. Astruc, W. Drexel, G. Gervais, W. Mampe, A new source of cold and ultracold neutrons, *Physics Letters A* 116 (7) (1986) 347 – 352.
- [23] F. Atchison, T. Brys M. Daum, P. Fierlinger, P. Geltenbort, R. Henneck, S. Heule, M. Kasprzak, K. Kirch, A. Pichlmaier, C. Plonka, U. Straumann, C. Wermelinger, First storage of ultracold neutrons using foils coated with diamond-like carbon, *Physics Letters B* 625 (2005) 19–25.
- [24] F. Atchison, B. Blau, M. Daum, P. Fierlinger, A. Foelske, P. Geltenbort, M. Gupta, R. Henneck, S. Heule, M. Kasprzak, M. Kuzniak, K. Kirch, M. Meier, A. Pichlmaier, C. Plonka, R. Reiser, B. Theiler, O. Zimmer, G. Zsigmond, Diamond-like carbon can replace beryllium in physics with ultracold neutrons, *Phys. Lett. B* 642 (2006) 24–27.
- [25] F. Atchison, A. Bergmaier, M. Daum, M. Doebeli, G. Dollinger, P. Fierlinger, A. Foelske, R. Henneck, S. Heule, M. Kasprzak, K. Kirch, A. Knecht, M. Kuzniak, A. Pichlmaier, R. Schelldorfer, G. Zsigmond, Surface characterization of diamond-like carbon for ultracold neutron storage, *Nuclear Instruments and Methods in Physics Research Section A* 587 (1) (2008) 82–88.
- [26] S. Gosh, N. Das, A. Mookerjee, Magnetic properties of Nio single-crystal

alloys; theory and experiment, *J. Phys.: Condens. Matter* 10 (1998) 11773–11780.

- [27] J. Bertsch, L. Göttl, K. Kirch, B. Lauss, R. Zubler, Neutron radiation hardness of vacuum compatible two-component adhesives, *Nuclear Instruments and Methods in Physics Research Section A* 602 (2) (2009) 552–556.